

A Simple, Adaptive Locomotion Toy-System

Jonas Buchli Auke Jan Ijspeert

Biologically Inspired Robotics Group (BIRG)

LSL, Swiss Federal Institute of Technology (EPFL), Lausanne

jonas.buchli@epfl.ch, auke.ijspeert@epfl.ch

<http://birg.epfl.ch>

Abstract

In order to successfully transfer biological principles to engineering problems, it is important to study the fundamental properties of biological systems. The goal is to arrive with useful abstractions that are (1) implementable, (2) testable by experiments and sample implementations, (3) retain the, for an engineering point of view, essential good properties of the biological systems. At BIRG, we are interested in the fundamentals of locomotion control and their possible applications to robotics. In this article, we present a simple, adaptive locomotion toy system that is of oscillatory nature. It is composed of two parts: an adaptive controller based on a nonlinear oscillator, and a mechanical system made of two blocks attached by an active and a passive spring. The controller is designed to be robust against perturbations, and to adapt its locomotion control to changing body kinematics or added external load. The tools to develop such a toy-system are a 2-scale nonlinear dynamical system, namely a Hopf oscillator with adaptive frequency, and an understanding of synchronization behavior of oscillators. A further central ingredient that will be discussed is the concept of asymmetric friction forces. We show that the system possesses several critical parameters. It is illustrated that the bifurcations connected with some of these parameters can be identified as non-smooth phase transitions and power law behavior. Links to biology and possible applications to robotics are discussed.

1. Introduction

Natural locomotion systems are of great interest for robotics as they present refined and robust solutions to a difficult engineering challenge. Namely, they manage to coordinate multiple degrees of freedom needed for locomotion, using signals of the right frequencies, phases and amplitudes (Ijspeert, 2003). However, any given natural locomotion system is of great complexity. In the case of a vertebrate locomotion system, it consists of an enormous number of muscle and neural cells and many other

types of body parts such as bones, tendons, etc. And even the locomotion apparatus of single cell organisms turns out to be of astonishing complexity (Marx, 2003).

However, as many people have pointed out, simple copying of biological processes can not be what we have to strive for when trying to enhance engineering principles by biological inspiration. It is rather the identification of the principles at a given level of abstraction that makes adaptation of biological principles for engineering problems successful (Buchli and Ijspeert, 2004).

Therefore, we have to look for fundamental principles underlying locomotion. In order to identify these principles, a broad range of locomotion systems have to be looked at. This includes single cell movement, worm, snail, snake, insect and mammalian locomotion, different types of flying and swimming but also more abstract concepts like active Brownian particles and ratchet systems.

When we try to find a few abstract principles common to all types of locomotion the following key observations arise:

- Locomotion is the process of transforming energy (unordered movement of many parts, particles) into directed movement (coordinated movement of the particles).
- From the first point we can directly conclude that locomotion always implies an active system and consumes energy¹.
- Any form of locomotion implies asymmetric interaction forces with the environment, e.g. an asymmetric friction mechanism (it turns out that this mechanism is what renders locomotion into a energy consuming process).
- Biological locomotion is robust, i.e. works under a very broad range of external (temperature, external forces, textures, ...) and internal (body properties, fatigue, sicknesses, ...) conditions. There are adaptation processes inherent in the locomotion systems to ensure this robustness.

¹The consumed energy can be potential energy (e.g. passive walkers) as well as energy from active mechanisms.

- The adaptation processes work on many, very different timescales. In other words, the time scales of, for instance, locomotion control, adaptation to fatigue, and adaptation to body development span over several orders of magnitude.

In order to make these fundamental principles accessible to theoretical and experimental investigation without the overhead of complicated experimental setups and difficult to control environments and subjects (all of which can easily hamper clear insight) we are looking for simple systems that, nevertheless, show all the properties listed above. Here we will report on a particular simple instance of a nonlinear dynamical system that possesses the described properties.

Modeling neuro-mechanical systems with oscillators During the last decades there have been growing numbers of attempts to model locomotion control systems with the help of oscillators (Buchli and Ijspeert, 2004). On the other hand bio-mechanical systems were modeled by spring mass systems or inverted pendulums - and are therefore of oscillatory nature (Blickhan, 1989, Full and Koditscheck, 1999). The logical consequence to model the complete neuro-mechanical systems by coupled oscillators has been used (Taga, 1995) and robotics controllers have been developed on the base of oscillators (Nakanishi et al., 2003). Oscillators are an important and widely used system to model phenomena in a broad range of fields. Often, simple oscillators with fixed parameters such as frequency and damping are used. Recently however, it was found that for modeling certain phenomena, oscillators with fixed frequencies are not sufficient. Therefore, oscillators with adaptive frequencies are investigated (Acebron and Spigler, 1998, Acebron and Spigler, 2000).

Exploiting adaptive frequency oscillators for locomotion control In this contribution we show that by using a Hopf oscillator with adaptive frequency we can devise a controller that adapts to the resonant frequencies of the mechanical system and therefore excites it. Together with asymmetric interaction forces with the environment - which turn out to be a fundamental property of any locomotion system - this leads to directed movement. There are 3 core ideas in our approach.

- The (bio)mechanical system is of oscillatory nature. I.e. it possesses resonant frequencies at which it can easily be excited.
- The controller is of oscillatory nature.
- The intrinsic frequency of the oscillator is adaptable and gets influenced by the mechanical system.

As we will see, by the proper choice of the mechanical system and the controller, a system that is self-exciting and adaptable can be devised. In order to convert the oscillatory movement of the mechanical system into directed movement a fourth fundamental property is necessary: The system needs some type of asymmetric interaction forces in our case asymmetric friction, i.e. the friction coefficients are lower for one direction compared to the other.

We use a simple mechanical spring-mass system to investigate the requirements needed for such a system to make directed movement. Furthermore, we are interested in a (simple) controller that is able to adapt to changing properties of the mechanical system (i.e. growth, mass changes, length changes).

2. A Simple, Adaptive Locomotion Toy-System

In order to study the aforementioned fundamental principles we devised a simple mechanical system controlled by an oscillator. We will describe the two main constituents of the system and their important properties along with how the two subsystems get connected in order to build the adaptive locomotion system.

Mechanical system The mechanical part of the system consists of two masses connected by two parallel springs S_a, S_p (cf. Fig. 1(a)), with different resting lengths l_a and l_p . For convenience, we will express them as $l_a = l_m + l_d$ and $l_p = l_m - l_d$, where l_m is the mean value and $2l_d$ the difference between both lengths. Both springs are linear springs with spring constant k_a, k_p . The system presented in this article is one-dimensional, in other words, the masses are assumed to move on, and remain in contact with, a horizontal plane and moving on a straight line. In the following, we present the mathematical description of such a system in terms of a system of differential equations. The system can be written as follows:

$$\dot{\mathbf{q}} = \mathbf{A}\mathbf{q} + F_c + F_r(\mathbf{q}) \quad (1)$$

where $\mathbf{q} = [x_1, v_1, x_2, v_2]^T$ are the state variables of the system (position and velocities of the two masses), \mathbf{A} is the matrix describing the action of the spring on the masses (without any friction), F_r is the friction present in the system and F_c is constant force arising from the differences and mean value of the resting length of the springs. \mathbf{A} takes the following form

$$\mathbf{A} = \begin{pmatrix} 0 & 1 & 0 & 0 \\ -\frac{k_a+k_p}{m} & 0 & \frac{k_a+k_p}{m} & 0 \\ 0 & 0 & 0 & 1 \\ \frac{k_a+k_p}{m} & 0 & -\frac{k_a+k_p}{m} & 0 \end{pmatrix} \quad (2)$$

where m are the masses attached at each end of the springs. And,

$$F_c = \frac{l_d(k_p - k_a) - l_m(k_a + k_p)}{m} [0, 1, 0, -1]^T \quad (3)$$

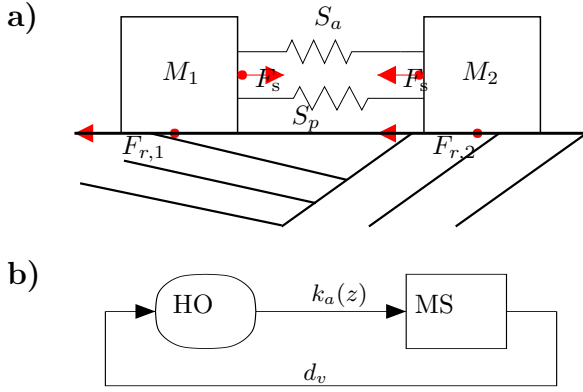


Figure 1: a) The mechanical sub-system of the adaptive locomotion toy system. It consists of two identical masses connected by a spring. From the mechanics of the system the forces acting on the body can be determined: F_s is the force that the springs exert on the blocks. It is of the same amplitude and opposite sign for the two masses. $F_{r,i}$ are the friction forces acting on the masses. With the help of these forces and Newton's law we are able to derive the system of differential equations that govern the mechanical system (Eq. 1). b) Schematic of the adaptive locomotion toy-system with its two main parts: The Hopf Oscillator (HO) and the spring mass system (MS). The Hopf Oscillator influences the mechanical system via the spring constant $k_a(z)$. The mechanical system in turn disturbs the Hopf oscillator by coupling in the velocity difference d_v as an additive disturbance to the Hopf Oscillator equations.

With the choice of l_m and l_d the resting position of the masses can be influenced. The choice of the friction term F_r will be discussed below. Such a second order linear system possesses a resonant frequency, which can be calculated as:

$$\omega_m = \sqrt{\frac{2(k_a + k_p)}{m}} \quad (4)$$

In other words, this type of mechanical system can be interpreted as a band pass filter with the pass band around ω_m . For generating displacements of the system, we replace the spring S_a described above with an active spring whose spring constant k_a can be modulated by a controller (see next section). The active spring can be seen as an abstract muscle-like actuator that can both pull and push.

Hopf oscillator As controller/activator of the mechanical system, we use a Hopf oscillator:

$$\dot{z} = (\mu_h + i\omega_h)z - |z|^2z + F(t), \quad z \in \mathbb{C} \quad (5)$$

which can be written in Cartesian coordinates:

$$\dot{x}_h = (\mu_h - r^2)x_h + \omega_h y_h + F_x(t) \quad (6)$$

$$\dot{y}_h = (\mu_h - r^2)y_h - \omega_h x_h + F_y(t) \quad (7)$$

where $x_h = \text{Re}(z)$, $y_h = \text{Im}(z)$ and $r = |z| = \sqrt{x_h^2 + y_h^2}$. ω_h is the intrinsic frequency of the oscillator and $F_x(t) = \text{Re}(F(t))$ and $F_y(t) = \text{Im}(F(t))$ are perturbing forces. The solutions of this system will be discussed below. The Hopf oscillator is coupled to the mechanical system in the following way (cf. Fig. 1(b)): First, the spring constant k_a is made a function of z in the following form:

$$k_a = k_0 + a \frac{x_h}{r} \quad (8)$$

where k_0 is a constant for the offset of the spring constant and a is a coupling constant, where $a < k_0$ to ensure S_a remains a spring ($k_a > 0$). Since x_h will be an oscillating term, this choice of coupling leads to an undulatory modulation of k_a , where the frequency of the modulation will be ω_h . The division by radius r serves to normalize the maximum of the modulation term to 1.

Second, the Hopf oscillator has feedback from the mechanical system:

$$F(t) = c d_v \doteq -c(v_1 - v_2) \quad (9)$$

where c is a coupling constant. Here, the choice has been on the considerations that mainly the coordination between the two bodies is important. Therefore, the choice of a difference term². The choice of the difference of velocities is chosen in order to have a more sensitive coupling in contrast to choosing the difference of positions³.

Properties of the Hopf Oscillator The Hopf oscillator acts as a frequency selective amplifier (Eguíluz et al., 2000), i.e. frequency components of $F(t)$ that are close to ω_h are amplified. Especially the setting $\mu_h = 0$ is special in the sense that the system undergoes a fundamental change at that point: For $\mu_h < 0$ the system exhibits a stable fixed point at $z = 0$, whereas for $\mu_h > 0$ a stable limit cycle occurs with radius $r = \sqrt{\mu_h}$. This phenomena is known as a Hopf bifurcation (Hopf, 1942). At $\mu_h = 0$, there is no signal oscillating at ω_h weak enough not to get amplified by the Hopf oscillator. Therefore, for that setting the Hopf oscillator can be considered an ideal amplifier⁴. This means that, if the resonant frequency ω_m of the mechanical system and the intrinsic frequency ω_h are close enough, any signal components close to the resonant frequency of the mechanical system get amplified. Thus, an excitation of the system can be expected.

In case of a biological setting, this would correspond to a case where the activation pattern of the muscles is well

²Such a difference is also more plausible from the practical and biological point of view, where no absolute values can play a role.

³It is expected, however, that with a proper choice of the coupling constant the qualitative behavior should not depend on this choice.

⁴We can not delve into the mathematical details of the Hopf oscillator in this contribution. For a more detailed treatment see e.g. (Kern and Stoop, 2003) and references therein.

adapted to the properties of the mechanical system, and, therefore, a very energy efficient mode of locomotion can be expected where only a small amount of energy has to be spent in order to maintain high locomotion velocity⁵. Animals possess adaptive processes which bring the locomotion system to (near) optimum mode of operation.

Adaptive frequency oscillator In our toy-system, adapting the oscillator to the mechanical systems means a proper choice or a tuning of ω_h . But, we can avoid manual tuning of ω_h by enhancing the dynamical system describing the Hopf oscillator. Instead of fixing ω_h we treat it as a variable with a corresponding differential equation describing the time evolution:

$$\dot{\omega}_h = f(\omega_h, q, t) \quad (10)$$

The choice of $f(\omega_h, q, t)$ that serves our purpose is chosen by understanding the synchronization behavior of two coupled oscillators. To get a good grasp on the effects of perturbations on a limit cycle system it is helpful to look at it in the phase plane representation (cf. (Strogatz, 1994)). In the phase plane all perturbations have a direction, i.e. they can be represented as a vector in that plane. It is known that a small perturbation of a limit cycle system can only affect that phase strongly if it perturbs the oscillator in direction tangential to the limit cycle, the perturbations perpendicular to the limit cycle are damped out⁶. Thus, depending on the state of the oscillator (the position of the phase point on the limit cycle) the perturbation accelerates the phase point or slows it down. If the perturbation is a periodic signal, with a frequency close to the intrinsic frequency of the oscillator, this results in an average acceleration or deceleration depending on the frequency difference and to synchronization. If we take this same effect to tune the frequency of the oscillator (on a slower time scale) the frequency should evolve toward the frequency of the perturbation. Therefore, the effect of $f(\omega_h, q, t)$ is the same as the effect leading to synchronization. Thus, (in average) driving ω_h toward ω_m . On that ground, we chose

$$\dot{\omega}_h = -\tau_h d_v \frac{y_h}{r} \quad (11)$$

where $\tau_h \ll 1$. However, the adaptation of ω_h happens on a slower time scale than the evolution of the rest of the system. This adaptation time scale is influenced by the choice of τ_h .

As explained, the output of the Hopf oscillator is coupled via setting $k_a = f(z)$ to the mechanical system. The

⁵Everybody knows this effect from sitting on a swing and trying to get it to move. If one moves the legs at the right frequency, with a minimum effort the swing can be brought to breathtaking heights.

⁶This is, of course, a simplification of the real facts. In fact, perturbations perpendicular to the limit cycle can, in general, perturb the phase of the oscillator. However, for the case of phase oscillators, such as the Hopf oscillator, the above simplification comes very close to the real thing. To discuss the general case is beyond the scope of this article.

mechanical system serves as a bandpass filter. Therefore, the Hopf oscillator, via the aforementioned feedback, slowly adapts its frequency to the mechanical system.

In order to measure the excitation of the system we can use the energy content of the mechanical part. There are two contributions to the energy of the mechanical system: The kinetic energy of the masses $E_k = \frac{1}{2}m(v_1^2 + v_2^2)$ and the potential energy of the springs $E_p = \frac{1}{2}(k_a(x_2 - x_1 - l_m + l_d)^2 + k_p(x_2 - x_1 - l_m - l_d)^2)$. We will use this formalism to investigate the optimal excitation frequency of the system in the next section.

Friction Friction dissipates the energy of the system. Therefore, if no energy is pumped into the system the system will always come to standstill from any initial condition. We have tested the system with two different friction schemes: viscous friction and Coulomb friction. Both are introduced as asymmetric friction forces, i.e. the parameters are lower for one direction compared to the other. In viscous friction, the friction force is proportional to the velocity of movement:

$$F_r = [0, -\rho_1 v_1, 0, -\rho_2 v_2]^T \quad (12)$$

where

$$\rho_i = \begin{cases} \rho_+ & \text{if } v_i > 0 \\ \rho_- & \text{if } v_i < 0 \end{cases} \quad (13)$$

The second model that has been tested is the Coulomb friction model, in which the friction coefficients are constant:

$$F_r = [0, F_{c,1}, 0, F_{c,2}]^T \quad (14)$$

$$F_{c,i} = \begin{cases} -|F_s| & \text{if } F_s < \mu_S |F_N| \text{ and } v_i = 0 \\ -\frac{v_i}{|v_i|} \mu_{r,i} |F_N| & \text{otherwise} \end{cases} \quad (15)$$

where $F_N = gm$ is the normal force of the body on the ground, and F_s is the spring force acting on the body. Coulomb friction has a static mode (when $v_i = 0$) and a dynamic mode. In our case, the dynamic friction is made asymmetrical as follows

$$\mu_{r,i} = \begin{cases} \mu_+ & \text{if } v_i > 0 \\ \mu_- & \text{if } v_i < 0 \end{cases} \quad (16)$$

With the Coulomb friction scheme the system would be unstable since the increase in the input of energy is increasing faster than the dissipation of energy due to friction. In order to avoid this instability problem, the coupling from the Hopf oscillator is slightly changed. The coupling constant a is made dependent on the rate of change of distance of the two masses, i.e. the velocity difference:

$$a_{coulomb} = \begin{cases} a & \text{if } |v_1 - v_2| < v_{thr} \\ 0 & \text{if } |v_1 - v_2| > v_{thr} \end{cases} \quad (17)$$

In other words, the coupling is switched off, if, due to heavy excitation the masses separate too fast. Thus, the

mechanical system runs passively for a short moment when reaching this maximum velocity until the spring forces and dissipation of energy bring it again below that threshold.

For this article the default friction model is the viscous model unless otherwise noted.

3. Simulation Results

The basic mode of locomotion is presented in Fig. 2(a). We show in vertical order consecutive snapshots of the mechanical system, at every 0.05 s. The locomotion of the system most closely resembles rectilinear-movement observed in some types of worms and snakes. The two masses exhibit an undulatory movement by which they are constantly stretching and compressing the springs between them. Due to the asymmetric friction forces one of the bodies is pushed (dragged respectively) toward one direction.

For the remainder of this section we would like to illustrate a few other important aspects of the presented locomotion toy-system. First, we list the parameters and initial conditions used in the simulations (unless otherwise noted):

Default parameter values				Default initial conditions	
parameter	value	parameter	value	variable	initial value
μ_h	0	l_m [m]	12	z	0
τ_h	0.1	l_2 [m]	0.5	ω_h [rads $^{-1}$]	12
c [sm $^{-1}$]	0.1	ρ_+ [Nsm $^{-1}$]	0.2	x_1 [m]	0
a [Nm $^{-1}$]	10	ρ_- [Nsm $^{-1}$]	0.1	v_1 [ms $^{-1}$]	0
m [kg]	1	μ_s	0.3	x_2 [m]	11.595
k_0 [Nm $^{-1}$]	10	μ_+	0.21	v_2 [ms $^{-1}$]	0
k_p [Nm $^{-1}$]	100	μ_-	0.19		
v_{thr} [ms $^{-1}$]	10				

In order to verify that the frequency calculated above is really the resonant frequency of the whole system (Hopf oscillator included) we make the following numerical experiment. We set $\tau_h = 0$, i.e. we go back to the fixed frequency oscillator. Then, we numerically integrate the system for different values of ω_h over a duration of 100 s. In Fig. 3, the resulting average energy content of the system is plotted against ω_h . The vertical lines depict the resonant frequency of the mechanical system and its 0.25, 0.5, 2,3 and 4 folds. As expected, the broadest peak is measured around the mechanical resonant frequency. Furthermore, there is a second strong peak (even higher amplitude but less broad) close to the harmonic $2\omega_m$. Apparently, the resonant effects at that point are very strong. Also around $0.25\omega_m$ and $0.5\omega_m$ resonant effects can be observed. They are however, much less strong. Furthermore, there seems to be a systematic shift of the resonant frequencies toward lower values for $\omega_h < \omega_m$ and toward higher values for $\omega_h > \omega_m$. In the lower panel the attained mean velocity of the center of mass is given. We see that that it follows the same pattern as the energy content of the mechanical system.

Henceforth, we introduce frequency adaptation into the Hopf oscillator by setting $\tau_h = 0.1$ and investigate

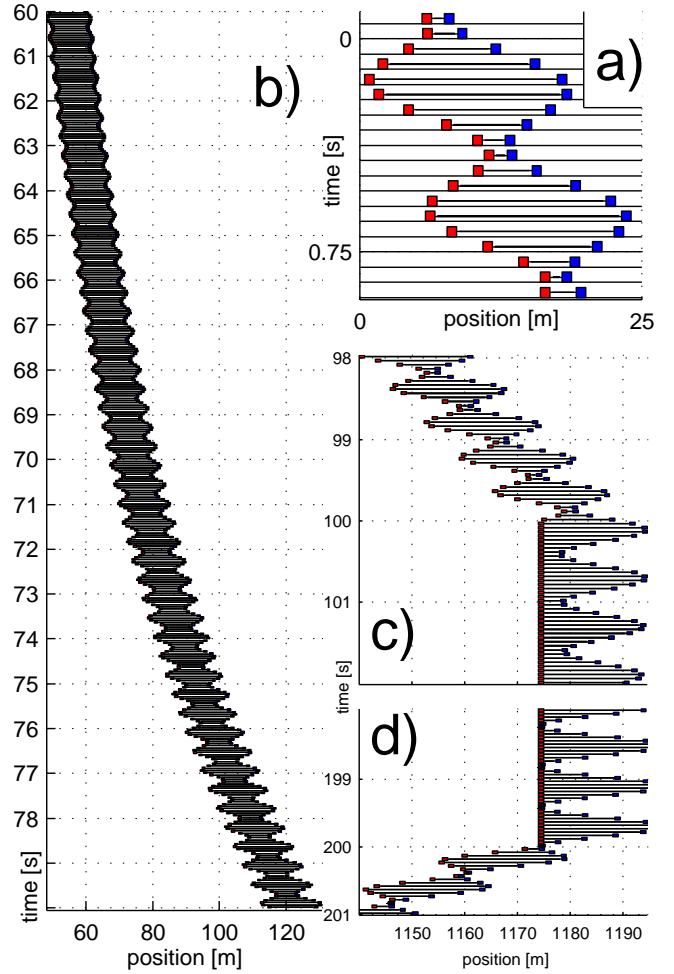


Figure 2: Illustration of the basic mode of locomotion. See text for description.

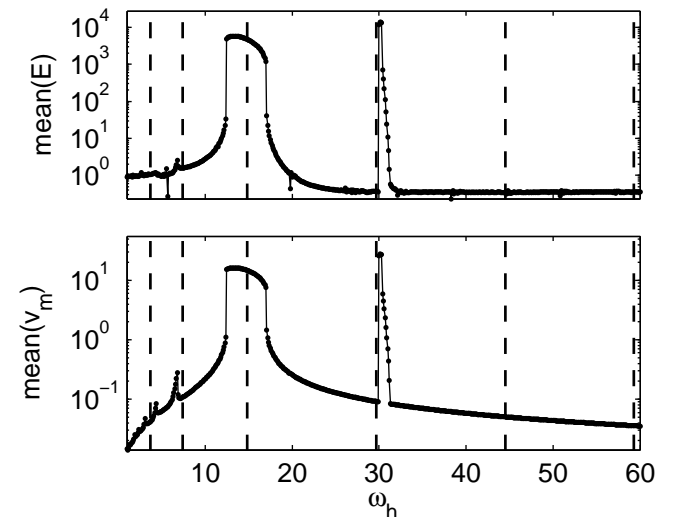


Figure 3: Top panel: Mean energy ($E_p + E_k$) content of the mechanical system for different $\omega_0 = [0, 60]$ at steady state. Bottom panel: Mean velocity. As clearly can be seen we have a broad peak around the resonant frequency of the mechanical system $\omega_m = 14.8324$.

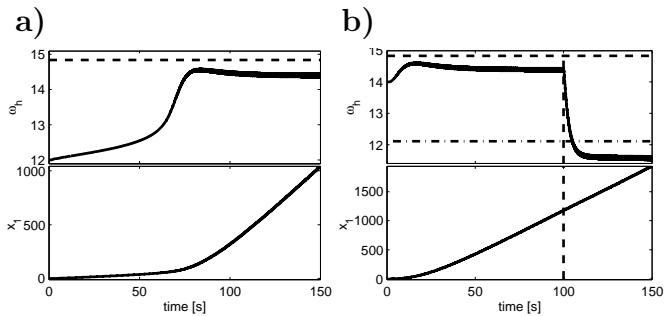


Figure 4: (a) This representative plot shows how the adaptation of ω_h increases the velocity of the locomotion system. ω_h starts at 12. The top panel shows the development of ω_h , the second panel shows the position x_1 of M_1 . There is some activity in the system from the beginning, however the excitations gets much stronger the closer ω_h comes to to the resonant frequency of the mechanical system ω_m (vertical line). The steady state for ω_h is around 14.4, which is lower then the calculated resonant frequency of the passive mechanical system: $\omega_m = 14.8324$.

(b) To illustrate the robustness that is built into the locomotion system by its frequency adaptation we show a representative experiment in which the mass of the bodies is 1kg to 1.5kg at $t=100$ s (vertical line). Immediately, the frequency of the oscillator ω_h starts to adapt to the new resonant frequency of the mechanical system (dash-dotted horizontal line).

the adaptation capability. We illustrate that the adaptation of ω_h leads to an increase of the forward velocity of the system. To get a first idea of how the system adapts ω_h and how this influences the speed of the mechanical system, we show a representative plot of ω_h and x_1 in Fig. 4(a) and the illustration of what happens with the masses from 60 to 80 seconds in Fig. 2(b). It can clearly be seen how the frequency adapts, first slowly then faster and finally reaches a steady state around $\omega_h = 14.4$. As can be seen the resonant effects start to excite the mechanical system heavily when ω_h passes at around 13 and the system starts to move forward at high speed.

In the next experiment, the mass is changed during the experiment at time $t = 100$ s from $m = 1$ kg to $m = 1.5$ kg. As we can see in Fig. 4(b) the oscillator quickly adapts its frequency to the new resonant frequency of the system and there is little change in the forward velocity. This corresponds for example to the biological case of growth of an animal or an addition of an external load. The adaptation to the massive change in the properties of the body immediately sets in, and after a few seconds the system has reached the new steady state.

As a further important aspect, the role of initial conditions of ω_h at $t = 0$ for the adaptation capability has been explored. As can be seen in Fig. 5, ω_h will always converge to the same value, but the initial conditions strongly affect the time ω_h needs to reach steady state. Furthermore, from the results in Fig. 3 we expect to

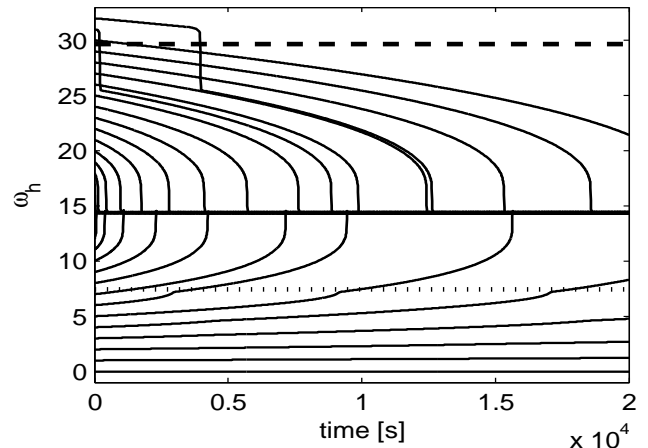


Figure 5: Adaptation of ω_h with viscous friction scheme. Different initial values for $\omega_h(0) = 0, 1, \dots, 32$ have been chosen. Clearly, the further away the longer ω_h takes to reach its stable steady state. The horizontal lines depict $0.5\omega_m$ and $2\omega_m$, where from the energy diagram (Fig. 3) resonant effects have to be expected and their influence on ω_h clearly can be observed here. Refer to text for further description.

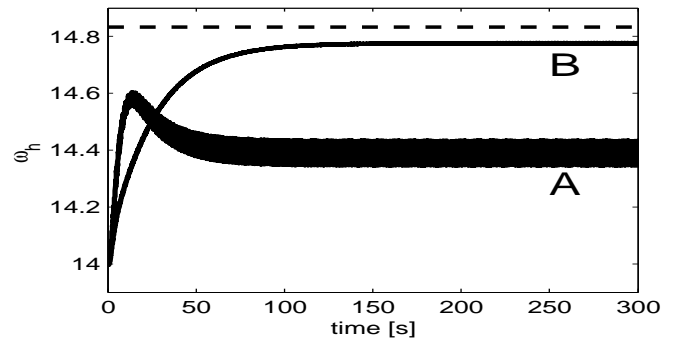


Figure 6: Comparison of the development of ω_h for viscous and Coulomb friction scheme. The Horizontal line indicates the resonant frequency of the passive mechanical system. (A) Viscous friction. (B) Coulomb friction. See text for further discussion.

see some clearly visible effects at $0.5\omega_m$ and $2\omega_m$ (the 1:2 and 2:1 resonant frequencies). At around $0.5\omega_m$ this leads to a slightly attractive area for ω_h (so called ghost points). Even more interesting is the effect at $2\omega_m$. From the energy diagram (Fig. 3) we know that the system reacts very strongly at that point. We can see that this violent reaction basically kicks the ω_h out of that region toward ω_m . So we see that even if the possible attained velocity is higher at $\omega_h = 2\omega_m$, this mode is not an attractor of the adaptation process.

Finally, in Fig. 6, a comparison between the viscous friction scheme and the Coulomb are presented. We see that the convergence for ω_h is slower in the case of the Coulomb scheme, and the final value is closer to the calculated resonant frequency of the passive mechanical system.

Influences of the Parameters Next, we want to shed light on the influence of the different parameters

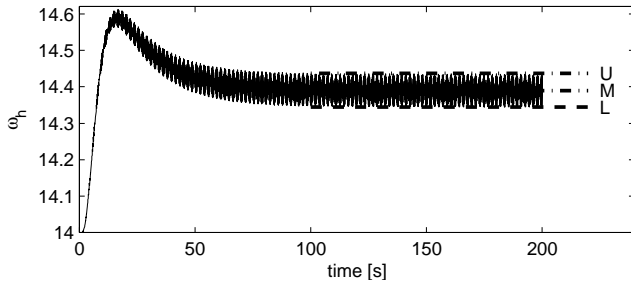


Figure 7: In order to quantify the steady state behavior of ω_h the mean m_{ω_h} and variance σ_{ω_h} have been measured after the system reached steady state (horizontal lines). Therefore, m_{ω_h} is a measure for (M) and σ_{ω_h} correlates with the distance (U)-(L). Note this figure is illustrative only – the actual values can change.

of the system. Note that the results in this section are of preliminary nature, since a lack of space and time does not allow to treat this topic in all detail in this article. There are a number of parameters which we can expect to influence the system fundamentally: First, the adaptation time scale of the Hopf oscillator τ_h directly influences the adaptation speed, but also the stability of the adaptation process. Second, the coupling constants between the Hopf oscillator and the mechanical system (a, c) can influence transient times as well as stability of the system. Third, the choice of the friction parameters ($\rho_+, \rho_-, \mu_r, \mu_s, \mu_d$) obviously influences the locomotion speed of the system.

The mechanical parameters, such as masses, resting distances and spring constants, which seem to be important at first sight, turn out to be not so fundamental in a second look. They merely determine the time and length scales on which the solutions will be found but do not influence the type of solutions that are possible.

We will now present results of numerical simulations, highlighting the influences of the parameters listed above. First of all, the behavior of the attained steady state values for ω_h depending on the choice of the coupling parameter c will be illustrated. The parameter c influences how strongly the mechanical system perturbs the Hopf oscillator. In order to quantify the dependence of ω_h on this (and other) parameters, we use the mean (m_{ω_h}) and variance (v_{ω_h}) of ω_h after it reached the steady state (cf. Fig. 7). These values are measures for location and shape (width/depth) of the attractor for ω_h .

In Fig. 8(a), can be seen that there is a bifurcation⁷ for a critical value of $c = C_c$. For $c < C_c$ there is a deviation of m_{ω_h} from the resonance frequency of the mechanical system ω_m . The deviation grows with an exponential increase in the variance when approaching C_c .

⁷Note that the names *bifurcation* and *phase transition* are basically two names for the same phenomena, even though with emphasis on different aspects. See (Haken, 1983) for a discussion.

At $c = C_c$ the mean and variance drop to 0, i.e. the system gets quenched. Such discontinuous behavior in the mean value and power law behavior of the variance are ubiquitous phenomena in phase transitions (bifurcations).

Next, we shed light on the influence of τ_h (cf. Fig. 8(b)) again we have a clear bifurcation behavior for a critical value of τ_h . For high values of $\tau_h > \tau_{h,c}$ it seems the system sets out onto a route into chaos (data not shown). The reason for that might be that for higher values of τ_h the timescales of the adaptation process and the other time scales of the system start to overlap, and therefore irregular behavior may occur. This conjecture however bases on visual inspection and is not confirmed yet. Again, we have a very clear power law behavior of σ_{ω_h} .

Now we turn our attention to the coupling from the Hopf oscillator to the mechanical system. The corresponding parameter is a . This parameter determines how strongly k_a is modulated by the activity of the Hopf oscillator (cf. Eq. 8). We measure the influence by calculating the mean value m_{v_1} of the attained velocity of M_1 at steady state. Here, we find a very clear linear dependence of m_{v_1} on a (cf. Fig 8(c)) for the explored range.

Finally, in Fig. 9, the influence of the friction asymmetry (ρ_+, ρ_n) is presented. After the transient phase the attained mean velocity of the center of mass is measured. As can be seen there is an exponential dependence of the velocity on the friction parameters.

Loss of feedback and disturbances It is also interesting to see how the system reacts when the feedback is cut from the mechanical system to the Hopf oscillator by setting $c = 0$. In Fig. 10(a), one can observe, that because of the setting of $\mu_h = 0$, the system keeps on moving, but at much reduced speed. If μ_h is set to slightly negative values $\mu_h = [-1, -10]$, the oscillations of the Hopf oscillator fade out and the system comes to a stand still (data not shown).

In a next step, we inhibit the frequency adaptation only by setting $\tau_h = 0$. In Fig. 10(b), can be seen how the system keeps on moving as normal, however it is not able to adapt to changing conditions anymore (data not shown).

In order to get an idea how the system behaves when it gets disturbed, we blocked one of the masses for 100 s. In Fig. 11, can be observed how the system reacts. Immediately the adaptation mechanism for ω_h starts to tune the system to the new resonant frequency $\omega_m = \sqrt{\frac{k_a + k_p}{m}}$. After releasing the blocks the system moves backward for a moment, before converging to the normal steady state again. What happens with the masses around $t = 100$ and $t = 200$ can also be seen in Fig. 2(c) and 2(d). Especially from Fig. 2(d) it can be understood where the

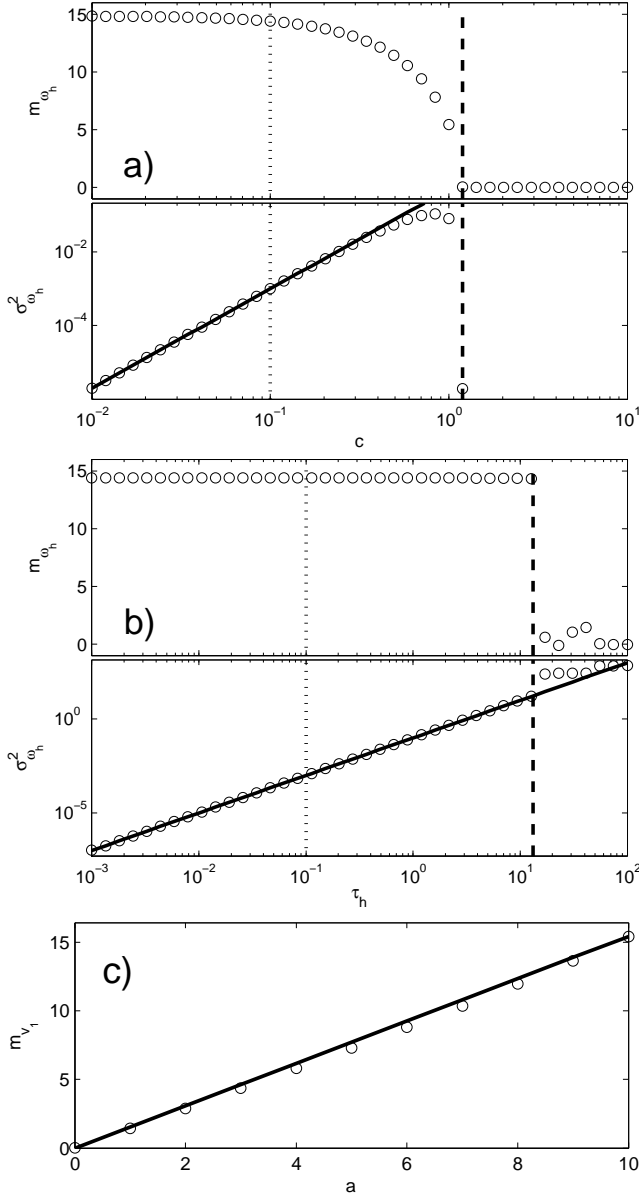


Figure 8: (a) Upper panel: the mean value attained for ω_h dependent on c (note the log scale). Lower panel: Variance for ω_h (note log-log scale). Note that for $c > C_c$ the variance drops to 0, therefore it is not drawn on the log scale. The vertical dotted line indicates the default setting of $c = 0.1$ and the dashed lines indicates the approximate value of C_c . The variance can be fitted with a power law $\sigma^2 \sim \tau^\alpha$. The exponent of the fit is $\alpha = 2.6959$. This behavior is typical for phase transitions.

(b) Dependence of mean and variance of ω_h on τ_h for steady state behavior. Again, the dotted line indicates the default setting of $\tau = 0.1$ and the dashed lines indicates the approximate value of $\tau_{h,c}$. The variance can be fitted with a power law $\sigma^2 \sim \tau^\alpha$. The exponent of the fit is $\alpha = 1.9903$. (c) The attained mean values m_{v_1} of v_1 after the system reached steady state depending on coupling parameter a . There is a very clear linear relationship $m_{v_1} = qa$. The fit is for $q = 1.5451$.

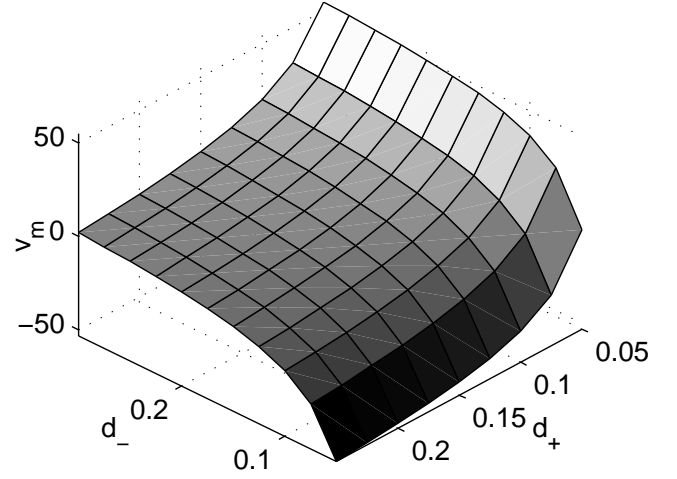


Figure 9: Influence of the friction asymmetry in viscous mode. The z axis is the position of m_1 after 200s for a given setting of ρ_- and ρ_+ . White regions correspond therefore to fast forward locomotion, black to fast backward locomotion.

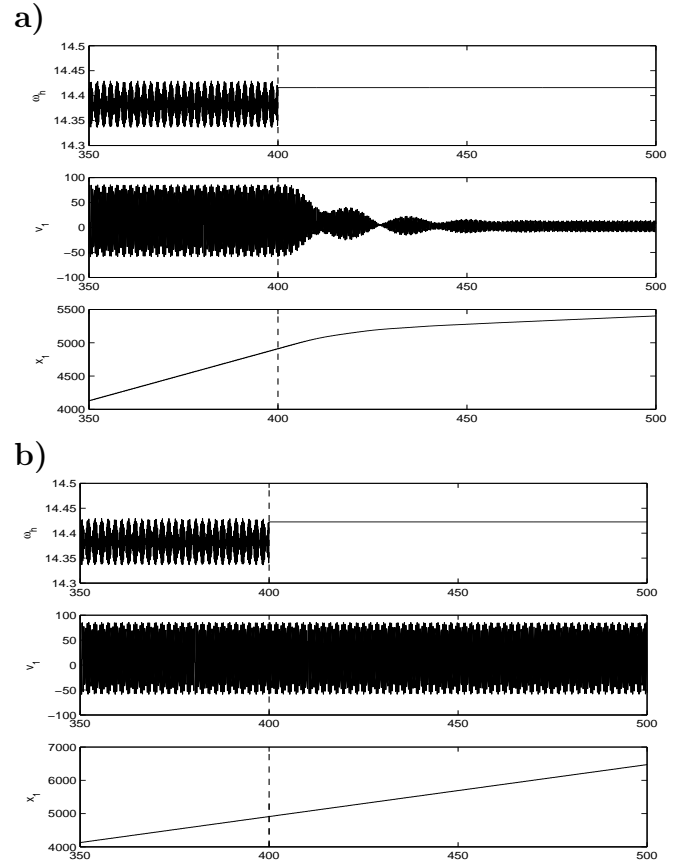


Figure 10: a) At $t = 400$ the feedback from the mechanical system to the Hopf Oscillator is cut by setting $c = 0$. This as well inhibits the frequency adaptation. b) At $t = 400$ only the frequency adaptation is cut by setting $\tau = 0$. This means there is still feedback from the mechanical system to the Hopf oscillator. Therefore, the system keeps moving with the same speed. However, it can not react to changing mechanical properties anymore (not shown).

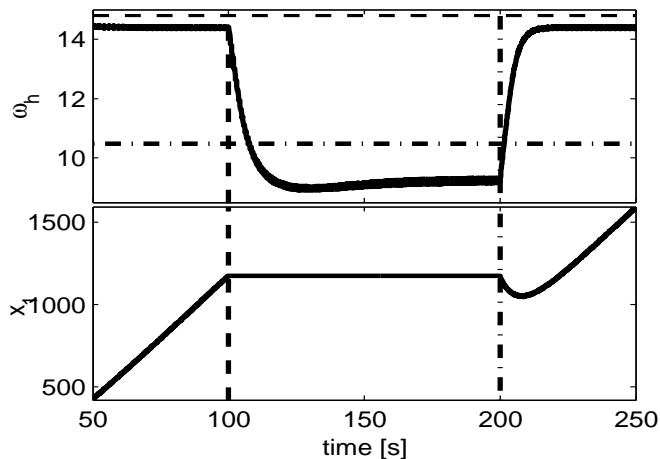


Figure 11: M_1 blocked at $t = 100$ (dashed vertical line) and released at $t = 200$ (dash dotted vertical line).

backward movement comes about. In the moment of the release of M_1 , M_2 happens to move with high velocity toward M_1 , which leads to acceleration backward in the moment of the release.

4. Discussion

In this article we have shown that, by using a Hopf oscillator with adaptive frequency, we can devise a controller that adapts to the resonant frequencies of a mechanical system and therefore excites it. We exploited the oscillatory nature of the systems and the understanding of synchronization behavior of oscillators. Together with asymmetric friction – which turns out to be a fundamental property of any locomotion system – this leads to directed movement. Asymmetric friction generalizes to asymmetric interaction forces for other types of locomotion, e.g. the elongated body of fishes have a low longitudinal and a large perpendicular drag coefficient, which by proper undulation of the body leads to forward movement. In the case of legged locomotion, the asymmetric interaction forces are implemented by having a stance phase with ground contact forces and a swing phase with zero interaction forces.

Two distinct time scales have been introduced into the dynamical system. Therefore, the system is a simple instantiation of a multi-scale⁸ dynamical system. The fast time scale is what normally is associated with the control of locomotion. The slow time scale can be associated with learning or, more generally, with adaptive behavior. Thus, we see the descriptive power that is naturally built into such multi-scale dynamical systems. Especially, there is no distinction between learning algorithm and learning substrate. Moreover, it is worthwhile noting that for a full understanding of the behavior of such a system, the two time scales can not be treated

⁸As a matter of fact it contains more than 2 time scales. Already a nonlinear oscillator possesses at least two time scales: One is the time scales of the oscillations and the other is the time scale at which it approaches its limit cycle.

completely separately.

Hitherto, multi-scale dynamical systems did not receive a lot of attention. One reason might be that there are some problems inherent in their investigation. One first problem that one encounters, is that, since there are many, possibly quite different, time scales in the system, the system has to be integrated in a way to encompass all time scales. In other words, the integration has to be exact enough (i.e. sampled fast enough) in order to calculate correctly the phenomena on the fastest time scale. On the other, hand the simulation has to run long enough in order to see the phenomena on the slowest time scale. The time scales are not fully separable since it is exactly the influence between them that is of interest. Furthermore, the interesting multi-scale systems usually exhibit strong nonlinear behavior and complicated bifurcation structure with many critical parameters, all of which makes it difficult the get a good understanding of the systems behavior. Recently, however, the interest in such systems is rising. One important reason is that cheap, fast workstations allow fast simulation of such systems and thus make their investigation more amenable.

Relation to biology We would like to stress the fact that the presented system is not meant to model detailed biological processes. It is rather a biologically inspired experimental system to investigate fundamental properties of locomotion (i.e. the generation of directed movement).

Nevertheless, and this is our hope, the treatment of such toy systems might lead to interesting questions for biologists. For instance, we have seen that our model reaches high velocities on higher order locking with the mechanical system. It would be interesting to see if the same phenomenon is observed in CPGs, and potentially, experimentally modify the CPG frequencies (e.g. through the application of excitatory neurotransmitters), and investigate whether it starts to work at these other resonant frequencies. In our case we saw a strong reaction, and it would be interesting to analyze the reaction of the natural system.

Furthermore, it is clear that the resonant frequencies of a locomotion system change very dramatically in an animal life time, and this at different time scales, e.g. due to the addition of external loads (e.g. carrying a prey) and to the growth of the animal. The natural locomotion systems have to cope with all such changes, and it would be interesting to explore the different types of adaptation mechanisms that play a role in keeping locomotion efficient. This is an area where the interplay between biology, engineering and mathematics can prove very fruitful.

Future work and outlook There are several avenues to build up on the presented results. First, there are

many theoretical questions that may be asked. Even if the system seems to be a quite simple one, the influence of the parameters is far from trivial. It will be interesting to further investigate the bifurcation behavior of the system. A careful investigation of the influence of the parameters remains to be done. We know that the system contains several critical parameters as outline above. In the presented results, most of them have been chosen in order to be on the safe side, e.g. τ_h has been chosen small enough in order to have two well separated time scales in the system.

Second, there are several extensions that can be made to the systems, such as an extension to non-oscillatory systems, for instance. We see that by exploiting synchronization behavior we can devise a useful system. On the other hand, there exist generalizations of the notion of phase locking and synchronization for aperiodic and non-oscillatory systems (Kuramoto, 1984). This could indicate that the presented approach is an interesting path to follow also for investigation of other problems, such as cognition, pattern recognition, evolutionary models and the like. Other extensions include introducing other coupling schemes and different types of oscillators.

The control of speed and direction also needs to be addressed. More springs and oscillators can be introduced in order to get a system that can change its direction of locomotion (2/3D system). Furthermore, the system should have some control over speed. Currently there is only stop and full speed (disregarding the transients between the two modes). However, a control of speed could be introduced, e.g. with an intentional detuning of the oscillator and/or with a modulation of the amplitude of oscillatory control signals. There are various other possibilities, of which the respective advantages and disadvantages and their implications on the system have to be carefully studied.

Finally, it would be interesting to construct a real-world robotics implementation of this toy-system as well as to implement it as a realistic dynamical simulation in a physics-based simulator. The system (most probably in a slightly modified form) should prove interesting for several robotics applications such as snake robots, (ad-hoc) modular robotics, and legged robots.

Acknowledgments This research is funded by a Young Professorship Award to Auke Ijspeert from the Swiss National Science Foundation. We would like to thank Jun Nakanishi for constructive comments on an earlier version of this article.

References

- Acebron, J. and Spigler, R. (1998). Adaptive frequency model for phase-frequency synchronization in large populations of globally coupled nonlinear oscillators. *Physical Review Letters*, 81:2229–2232.
- Acebron, J. and Spigler, R. (2000). Uncertainty in phase-frequency synchronization of large populations of globally coupled nonlinear oscillators. *Physica D*, 141(1–4):65–79.
- Blickhan, R. (1989). The spring-mass model for running and hopping. *J. Biomechanics*, 22(11–12):1217–1227.
- Buchli, J. and Ijspeert, A. (2004). Distributed central pattern generator model for robotics application based on phase sensitivity analysis. In *Proceedings Bio-ADIT2004*, Lecture Notes in Computer Science. Springer Verlag Berlin Heidelberg. To appear, preprint at <http://birg.epfl.ch>.
- Eguíluz, V., Ospeck, M., Choe, Y., Hudspeth, A., and Magnasco, M. (2000). Essential nonlinearities in hearing. *Phys Rev Lett*, 84(22):5232–5235.
- Full, R. and Koditscheck, D. (1999). Templates and anchors: neuromechanical hypotheses of legged locomotion on land. *Journal of Experimental Biology*, 202:3325–3332.
- Haken, H. (1983). *Synergetics. An introduction*. Springer Verlag Berlin Heidelberg, 3rd edition.
- Hopf, E. (1942). Abzweigung einer periodischen Lösung von einer stationären Lösung eines Differentialsystems. *Ber. Math.-Phys., Sächs. Akad. d. Wissenschaften, Leipzig*, pages 1–22.
- Ijspeert, A. (2003). Vertebrate locomotion. In Arbib, M., (Ed.), *The handbook of brain theory and neural networks*, pages 649–654. MIT Press.
- Kern, A. and Stoop, R. (2003). Essential role of couplings between hearing nonlinearities. *Physical Review Letters*, 91.
- Kuramoto, Y. (1984). *Chemical oscillations, Waves, and Turbulence*. Springer Verlag Berlin Heidelberg.
- Marx, J. (2003). How cells step out. *Science*, 302(5643):214–216. Science News Focus. Cell Biology.
- Nakanishi, J., Morimoto, J., Endo, G., Cheng, G., Schaal, S., and Kawato, M. (2003). Learning from demonstration and adaptation of locomotion with dynamical movement primitives. *Special issue of Robotics and Autonomous Systems*. To appear.
- Strogatz, S. (1994). *Nonlinear Dynamics and Chaos*. Addison Wesley Publishing Company.
- Taga, G. (1995). A model of the neuro-musculo-skeletal system for human locomotion. I. Emergence of basic gait. *Biological Cybernetics*, 73(2):97–111.